

## Journal Pre-proof

Effect of process parameters in high shear granulation on characteristics of a novel co-processed mesoporous silica material



Ana Baumgartner , Odon Planinšek

PII: S0928-0987(23)00158-6  
DOI: <https://doi.org/10.1016/j.ejps.2023.106528>  
Reference: PHASCI 106528

To appear in: *European Journal of Pharmaceutical Sciences*

Received date: 31 January 2023  
Revised date: 12 July 2023  
Accepted date: 12 July 2023

Please cite this article as: Ana Baumgartner , Odon Planinšek , Effect of process parameters in high shear granulation on characteristics of a novel co-processed mesoporous silica material, *European Journal of Pharmaceutical Sciences* (2023), doi: <https://doi.org/10.1016/j.ejps.2023.106528>

This is a PDF file of an article that has undergone enhancements after acceptance, such as the addition of a cover page and metadata, and formatting for readability, but it is not yet the definitive version of record. This version will undergo additional copyediting, typesetting and review before it is published in its final form, but we are providing this version to give early visibility of the article. Please note that, during the production process, errors may be discovered which could affect the content, and all legal disclaimers that apply to the journal pertain.

© 2023 Published by Elsevier B.V.  
This is an open access article under the CC BY-NC-ND license  
(<http://creativecommons.org/licenses/by-nc-nd/4.0/>)

## Highlights

- Granulation of mesoporous silica and isomalt yields co-processed excipient
- Co-processed silica exhibits improved properties compared to the starting material
- Granulation process parameters greatly influence characteristics of the excipient
- Design of Experiment method gives a good insight into factors governing granulation

Journal Pre-proof

**RESEARCH ARTICLE**

Effect of process parameters in high shear granulation on characteristics of a novel co-processed mesoporous silica material

Ana Baumgartner\*, Odon Planinšek

Faculty of Pharmacy, University of Ljubljana, 1000 Ljubljana, Slovenia

**\*Corresponding author: Ana Baumgartner**

Faculty of Pharmacy

University of Ljubljana

Aškerčeva 7

1000 Ljubljana, Slovenia

Email: ana.baumgartner@ffa.uni-lj.si

Tel: +386-1-4769690

## Abstract

In this study, insights into the development and optimization of a co-processed excipient based on mesoporous silica are presented. The main advantage of such a material is that it is appropriate for direct tablet compression and has a sufficiently large specific surface area to be suitable for potential subsequent drug loading and formulation of (amorphous) solid dispersions. Our aim was to use a Design of Experiments approach to investigate which process parameters in high shear granulation affect the characteristics of such a co-processed material. The parameters included were the amount of binder (isomalt), the amount of water (granulation liquid), the water addition rate and the speed of the impeller. The responses evaluated and modelled were particle size and its distribution, specific surface area, bulk density, flowability, compressibility and compactibility. The models obtained showed good quality in terms of goodness of fit and predictive power. Active effects were identified for all responses, giving a thorough insight into factors affecting the material characteristics. Optimization experiments resulted in products with the desired characteristics (high specific surface area, large particle size, good flow and compression properties) and confirmed the validity of the generated models.

Keywords: mesoporous silica, high-shear granulation, Design of Experiment, co-processing, excipient

List of abbreviations

API	Active pharmaceutical ingredient
MCC	Microcrystalline cellulose
DoE	Design of Experiment
SEM	Scanning electron microscope
PVP	Polyvinyl pyrrolidone
SSA	Specific surface area
w	Amount of water
war	Water addition rate
bind	Amount of binder
imp	Impeller speed

## 1 Introduction

Despite the development of various novel dosage forms and drug delivery systems in recent years, tablets are still the most commonly used due to their stability, dose uniformity and patient acceptability (1). They are usually manufactured by wet granulation, dry granulation, or direct

compression. While the first two approaches require several intermediate processing steps to prepare granules prior to tablet compression, direct compression consists only of simple blending of the powder components and compressing them. Therefore, this approach is considered less complicated and less time-consuming and costly, and unlike indirect compression methods, it also avoids heat and moisture effects (1–3). However, its use is often hindered by suboptimal compression properties, flow properties and dilution potential of the active pharmaceutical ingredient (API) (1,4). Therefore, the API content in such tablets is usually limited to 30%, which is referred to as “low dilution potential”. In addition, particle segregation often occurs during the mixing process, which can negatively affect content uniformity (2,3).

Excipients play a crucial role in controlling or improving tableting properties, especially if their content is high enough (5). Therefore, the choice of excipients is of utmost importance in direct tableting. The events that occur during the tablet compression cycle are initial packing and rearrangement of particles, formation of temporary structures, elastic and plastic deformation, breakage of the particles, bond formation, consolidation and in the end elastic recovery during decompression. When it comes to direct powder compression, it is important to study the compressibility (ability to undergo volume reduction under pressure) and compactibility (ability to compact with adequate strength) of the material in addition to the flow properties, which have to be good enough to ensure homogeneous and rapid flow of the powder in the die (6,7). Excipients with improved performance with respect to these properties can be obtained either as new chemical entities, improved grades of existing materials or by processing two or more excipients without altering their chemical structure, also referred to as co-processing (1,4). The development of a new chemical excipient is costly, laborious, and complicated from a regulatory perspective, while improved grades of existing excipients (microcrystalline cellulose (MCC), spray-dried mannitol, etc.) often have limited performance (8). On the other hand, co-processed excipients have been developed to avoid these problems.

As defined by the International Pharmaceutical Excipients Council, a co-processed excipient is a combination of two or more compendial or non-compendial excipients designed to physically modify their properties in a manner not achievable by simple physical mixing, and without significant chemical change (9). Co-processed excipients are often prepared by spray-drying, wet granulation or co-crystallisation. These methods cause the individual excipients to interact at the sub-particulate level, which leads to improved characteristics of the product material compared to those of individual components. Other main advantages of co-processed excipients are the elimination of wet granulation production steps, the avoidance of handling multiple excipients, and the acceleration of new product launches without time-consuming and costly testing (1,4,8,10).

The concept of co-processing was first introduced in 1988 with a patent granted to co-processed MCC and calcium carbonate (11). Since then, many co-processed excipients have been developed for direct tableting as well as for some other more specific uses, such as the formulation of orally disintegrating tablets. Some of these materials are described in more detail in Table 1, but it must be acknowledged that this is only a small selection of those available.

Table 1: Examples of co-processed excipients on the market

<b>Excipient name</b>	<b>Individual components and their content</b>	<b>Advantages, intention of use</b>	<b>References</b>
<b>Cellactose®</b>	α-lactose monohydrate (75%) Powdered cellulose (25%)	Improved flowability and compactibility Direct compression	(12)
<b>Ludipress®</b>	Lactose monohydrate (93%) Kolidon®30 (3.5%) Kollidon®CL (3.5%)	Improved flowability and tableability, rapid disintegration Direct compression	(13)
<b>StarLac</b>	Maize starch (15%) α-lactose monohydrate (85%)	Improved flowability, rapid disintegration Direct compression	(14)
<b>Ludiflash®</b>	D-Mannitol (84-92%) Kollidon®CL-SF (4-6%) Polyvinyl acetate (3.5-6%) Kollidon®30 (0.25-0.60%) Water (0.5-2.0%)	Rapid disintegration, pleasant taste Direct compression, fast disintegrating solid oral dosage forms	(15,16)
<b>Pharmaburst® 500</b>	D-Mannitol (85%) Silicon dioxide (<10%) Sorbitol (<10%) Crospovidone (<5%)	Rapid disintegration, good compaction, good mouthfeel Orally disintegrating tablets	(10,17)

It can be seen that existing co-processed excipients often use similar materials and that their main purposes of use are direct compression and formulation of fast disintegrating tablets. However, in this study, we introduce a novel co-processed excipient consisting of two materials rarely found in previously developed co-processed excipients, namely mesoporous silicon dioxide and a sugar alcohol isomalt, which according to the chemical structure is a disaccharide alcohol 1-O-D-

glucopyranosyl-D-mannitol dihydrate (1,1- GPM dihydrate) and 6-O-D-glucopyranosyl-D-sorbitol (1,6- GPS) (18).

The main reason for using mesoporous silicon dioxide, i.e. silica, is its high specific surface area (i.e., up to 500 m<sup>2</sup>/g) and high pore volume (i.e., >1 cm<sup>3</sup>/g), which is why it is possible to achieve adsorption of drugs on this material and thereby formulate (amorphous) solid dispersions. If the adsorbed drug is otherwise poorly soluble in water, a larger surface area as well as the amorphous state may contribute to its faster dissolution and/or higher solubility (19). This is particularly important considering that poor water solubility is a major challenge in pharmaceutical research and industry (20). On the other hand, silica has low bulk density as well as small and irregularly shaped particles, which results in poor powder flow behaviour and makes it inappropriate for direct tableting. However, if such particles are agglomerated by granulation, these properties can be improved (21,22). By definition, granulation means that the particles are agglomerated into larger aggregates (granules) in which the original particles can still be recognised (23). Although agglomeration of particles results in a decrease in specific surface area (SSA), the large SSA of the starting mesoporous material is still expected to guarantee a sufficiently large surface area of the granulated product to be suitable for drug adsorption.

There have been some attempts to granulate poorly flowing mesoporous silica into a more flowable and compressible material. Vialpando et al. (24) attempted to granulate mesoporous silica material COK-12, previously loaded with various poorly water-soluble drugs, by wet granulation using polyvinylpyrrolidone (PVP) as a binder solution to improve bulk flow properties and compactibility of solid dispersion. Comparison with pure COK-12 showed that increasing the particle size improved the powder flow properties and compactibility. In another study, they attempted to granulate COK-12 (mesoporous silica with ordered pore network) and Syloid® 244 FP (mesoporous silica with disordered pore network) loaded with itraconazole by melt and steam granulation. Poloxamer 188 and PVP K25 were used as binders for melt and steam granulation, respectively. They successfully achieved increased bulk density and improved flow behaviour as shown by Carr index (21,22).

In our co-processed material, the substance used to bind silica particles into granules is isomalt. Sugar alcohols are becoming more and more interesting as pharmaceutical excipients due to their pleasant taste, low caloric content, non-cariogenic properties and good stability. However, they are not always suitable for direct compression without any physical modification, but isomalt has been shown to have a positive effect on compactibility and compressibility due to its binder properties (18,25). In addition, sugar alcohols are very poorly soluble in organic solvents, which is another desirable property especially for our co-processed material. Indeed, if a poorly water-soluble drug is

to be adsorbed onto the described co-processed material, the most common approach used at the laboratory scale is adsorption from a drug solution in an organic solvent in which the granules should not dissolve or disintegrate(26,27).

In our case, high shear wet granulation was used to co-process silica and isomalt. In this method, particle size is achieved by adding liquid to the powders during mixing in a high-shear mixer (28,29). Although high-shear granulation is widely used in the pharmaceutical industry because of its short manufacturing time and good product quality, it is still considered a complex process with many parameters that affect the properties of the final product (30,31). To investigate and better understand the effect of process parameters on product characteristics, a Design of Experiment (DoE) approach can be used, because it can help in the development of a high-quality product by reducing the number of experiments (28). There are several studies (28,29,31–33) in which scientists have successfully applied DoE approach to better understand the process of high shear granulation. However, it has been found that the question of which parameters are most important and how they affect the final product is case-specific.

In the present study, we use DoE approach to investigate which process parameters in high shear granulation affect the characteristics of the above-described novel co-processed material. The desired characteristics should be such that they result in a product that is both suitable for direct compression and has a large enough SSA for subsequent investigations pertaining to drug loading and amorphous solid dispersion formulation.

## 2 Materials and methods

### 2.1 Materials

Isomalt (GalenIQ 800) was kindly donated by Beneo (Germany). Mesoporous silica (Syloid 244 FP) was obtained from Grace Davison, Grace GmbH & Co. KG (Germany). Magnesium stearate was obtained from Merch KGaA (Germany). Water was purified by reverse osmosis.

### 2.2 Methods

#### 2.2.1 High shear granulation

Co-processed excipient was made by wet granulation in a high-shear mixer (ProCepT 4M8-Trix, Belgium). Silica and isomalt were added to a 1 L glass vessel. The blend was first stirred for two minutes at impeller speed 125 rpm. Then distilled water was added dropwise at a specified flow rate. During water addition, the speed of the chopper was set at 1000 rpm and the speed of the impeller was set as specified in the experimental design. After complete liquid addition, granulate was sieved through a 2 mm sieve using a plastic card and dried on trays at 60 °C until the moisture



content was below 2% (determined by loss-on-drying test), i.e. 3-4 hours. Dried granulate was sieved through a 710  $\mu\text{m}$  sieve, and particles passing 80  $\mu\text{m}$  sieve were discharged.

Loss-on-drying tests were performed at 85 °C for 15 minutes (until constant weight) using an infrared moisture analyzer (B-302; Buchi, Switzerland), with approximately 2 g of the sample placed on an aluminium plate.

The percent yield of each sample was calculated using Eq. 1:

$$Y = \frac{m(\text{dried product})}{m(\text{silica})+m(\text{isomalt})} \quad (\text{Eq. 1})$$

where  $m(\text{dried product})$  represents the mass of the dried and sieved granulate.

### 2.2.2 Particle morphology

Particle morphology was studied by scanning electron microscope (SEM). The particles were deposited on a double-sided carbon tape (diameter 12 mm, Oxon, Oxford Instruments, UK). A SEM (Supra 32 VP, Zeiss, Germany) with an accelerating voltage of 1.00 kV and a secondary detector was used. The samples were scanned with a magnification of 250x.

### 2.2.3 Particle size

Particle size parameters  $d_{10}$ ,  $d_{50}$  and  $d_{90}$  (volumetric parameters indicating the fraction of particles smaller than 10%, 50%, and 90%, respectively) were measured using laser diffraction method (Malvern Mastersizer 3000, Malvern Instruments, UK) with a dry powder feeder. The following parameters were used: feed air pressure 1 bar, 0.5–6% obscuration rate and Fraunhofer approximation theory setting. Each sample was measured in triplicate. The width of the particle size distribution (span) was calculated using Eq. 2:

$$\text{span} = \frac{d_{90}-d_{10}}{d_{50}} \quad (\text{Eq. 2})$$

### 2.2.4 Bulk density and flow properties

Bulk volume and density were determined by gently pouring the weighed sample into a dry 100 mL cylinder. The sample was mechanically tapped 1250 times (Vankel Tap Density Tester, VanKel, NC) to determine tapped volume and density. Each sample was measured in triplicate.

Flow properties were determined in accordance with the European Pharmacopoeia, 10<sup>th</sup> edition, by calculating the Hausner ratio (34). Each sample was measured in triplicate.

### 2.2.5 Specific surface area

SSA was determined via nitrogen adsorption isotherms (Nova 2000, Quantachrome Instruments, USA). Calculation of SSA was based on the multipoint Brunauer-Emmett-Teller equation (BET) in the relative pressure range of 0.05 to 0.3 (35). Each sample was measured in duplicate.

The total pore volume was estimated using the t-plot method (36). The pore-size distribution and average pore radius was derived from the adsorption branches of the nitrogen isotherms using the BJH (Barrett-Joyner-Halenda) model (37). Adsorption and desorption isotherm plots were acquired via OriginPro 2018 software (OriginLab Corporation, USA).

Prior to measurements, the samples were kept under vacuum at 70 °C overnight. Between 0.5 and 1 g of the sample was used for each measurement.

### 2.2.6 Compressibility and compactibility

For each mixture, 10–15 tablets were compressed at various compression pressures ranging from 20 MPa to 150 MPa using a single-punch tablet press (Kilian SP300, IMA, Germany) with round flat-faced punches ( $d = 12$  mm). Magnesium stearate (0.5%  $m/m$ ) was added as antiadhesive-agent. Compression speed was 25 tbl/min and the target tablet mass was 500 mg. Tablets were weighted immediately after compression (Sartorius, Germany), however, the other characteristics were evaluated 24 hours after compression; thickness and diameter were measured with a micrometer (Mitutoyo, Japan), and tablet crushing force was evaluated with a hardness tester (Kraemer Elektronik, Germany). True density of the tablets was determined in triplicate with a helium pycnometer (AccuPyc 1330, Micromeritics, USA) according to European Pharmacopoeia, 10<sup>th</sup> edition.

Compressibility was determined using the “out-of-die” Heckel compressibility model, which is based on the premise that the process of pore reduction during compression follows first-order kinetics, as shown in Eq. 3:

$$-\ln \varepsilon = \ln\left(\frac{1}{1-D}\right) = K * P + A \quad (\text{Eq. 3})$$

where  $\varepsilon$  is porosity,  $D$  is relative density of the compact (calculated from tablet mass and volume),  $P$  is applied pressure, and  $K$  (referred to as the Heckel constant) and  $A$  are regression coefficients of the linear portion of the curvature. Yield pressure ( $P_y$ ), which is the reciprocal value of Heckel constant, is a measure of compressibility and plasticity of the material (38).

Compactibility was determined by plotting tablet tensile strength against compaction pressure. Tensile strength ( $\sigma_T$ ) was calculated using Eq. 4:

$$\sigma_T = \frac{2H}{\pi dh} \quad (\text{Eq. 4})$$

where  $H$  is tablet crushing force,  $d$  is the diameter and  $h$  is the thickness of the tablet. The slope of the linear portion of the curvature was denoted as  $c_p$  and used as a measure of compactibility (38).

### 2.2.7 Experimental design

Experimental design was performed using Modde® 13.0.2 software (Sartorius, Germany). Preliminary experiments were conducted to determine which process parameters were critical for product properties and to select an appropriate range for these parameters. Based on the results of these experiments, four main parameters (factors) were selected: the amount of isomalt as binder, the amount of water as granulation liquid, water addition rate, and impeller speed. Central composite orthogonal experimental design was used to obtain the models, meaning that each factor was varied at five different experimental design points: (a) two-level fractional factorial design points (coded as +1 and -1), (b) center points, representing the middle value between +1 and -1 and used to estimate replicability (coded as 0), and (c) axial points representing new extreme values of each factor while others are kept at middle value (coded as  $+\alpha$  and  $-\alpha$ ) (39). The coded values of each factor are shown in Table 2. The amount of silica was kept constant, i.e., 30 g, to keep the filling of the glass vessel for granulation as constant as possible; since silica is a very voluminous powder, the effect of the amount of binder on the vessel filling is negligible. Chopper speed in the granulator was also kept constant at 1000 rpm.

Table 2: Factors and their coded values

Factor	Unit	$-\alpha$	-1	0	+1	$+\alpha$
Isomalt amount	g	13.6	15	17.5	20	21.4
Water amount	g	67.3	70	75	80	82.7
Water addition rate	g/min	1.2	1.8	2.8	3.8	4.2
Impeller speed	rpm	30	50	125	200	241

A total of 27 experiments were performed, among which 3 were repetitions at the center point of the DoE, meaning that all factors were set at value 0. Responses that were taken for modelling and optimization were particle size parameters ( $d_{10}$ ,  $d_{50}$ ,  $d_{90}$  and span), SSA, bulk density, compressibility (assessed by yield pressure), compactibility (assessed by  $c_p$ ) and Hausner ratio. A stepwise regression (partial least squares method) with an alpha of 0.05 was used to get a hierarchical model with the best predictive performance, expressed as  $Q^2$ , which was achieved by iterative process of eliminating the non-significant variables for each response. Non-significant variables were included in some models either to keep them hierarchical or to ensure the highest possible  $Q^2$ . A  $Q^2$  greater than zero indicates that the model is significant, and if it exceeds 0.5, the

model is considered to have good predictive ability. Other parameters that were calculated to estimate the quality of the models were goodness of fit ( $R^2$ ), reproducibility, and validity. For a good model,  $R^2$  should be as close to 1 as possible and should not deviate more than 0.3 from  $Q^2$ . To avoid the lack-of-fit of the model, validity should be greater than 0.25. Reproducibility should also be close to 1 (40).

Optimization experiments were conducted to optimize either individual responses or two responses at once. In optimization experiment #1, particle size and SSA were optimized to a maximum value, in optimization experiment #2, yield pressure as a measure of compressibility was optimized to a minimum. The process parameters for optimization experiments were determined with the response optimizer in Modde® software.

### 3 Results and discussion

A total of 27 experiments were performed, but only 20 acceptable granulates were obtained and characterized due to overwetting which occurred in some experiments and prevented further handling of the product. The results are shown in Table 3. As can be seen, the process yield was above 90% in 11 out of 20 cases, while only one experiment gave a yield below 70% (N19). Considering that part of the starting material always remained ungranulated and was discarded as dust fraction, the process yield was still quite satisfactory.

Table 3: Responses for each performed experiment. For responses with multiplied measurements, average values are given. Blue squares indicate that the experiments could not be performed due to inappropriate materials (over-wetting). Grey squares indicate values that have been excluded from model fitting as they were outliers.

Experiment Name	Input variables					Responses									
	water amount (g)	water addition rate (g/min)	impeller speed (rpm)	isomalt amount (g)	Total dry powder amount (g)	yield (%)	d10 (um)	d50 (um)	d90 (um)	span	bulk density (g/mL)	Hausner ratio	SSA (m <sup>2</sup> /g)	P <sub>v</sub> (MPa)	c <sub>p</sub>
N1	70	1.8	50	15	45	82.0	6.4	238	669	2.78	0.26	1.31	141	260.7	0.011
N2	80	1.8	50	15	45	72.4	66.7	406	854	1.94	0.38	1.18	161	395.1	0.007
N3	70	3.8	50	15	45	94.7	3.5	207	583	2.80	0.25	1.40	144	389.6	0.027
N4	80	3.8	50	15	45	79.7	11.5	279	635	2.23	0.27	1.41	142	434.2	0.022
N5	70	1.8	200	15	45	78.7	121	481	929	1.68	0.38	1.29	147	505.8	0.011
N6	80	1.8	200	15	45										
N7	70	3.8	200	15	45	94.1	43.6	356	775	2.05	0.32	1.28	145	345.4	0.033
N8	80	3.8	200	15	45										
N9	70	1.8	50	20	50	94.3	7.2	281	686	2.42	0.29	1.33	115	237.3	0.026
N10	80	1.8	50	20	50	91.2	45.8	384	800	1.96	0.33	1.27	111	339.9	0.029
N11	70	3.8	50	20	50	94.4	3.6	229	685	2.98	0.27	1.43	92	221.5	0.017
N12	80	3.8	50	20	50	94.3	4.6	230	705	3.05	0.33	1.33	113	239.2	0.012
N13	70	1.8	200	20	50										
N14	80	1.8	200	20	50										
N15	70	3.8	200	20	50	95.5	41.4	360	802	2.11	0.35	1.26	100	236.6	0.017
N16	80	3.8	200	20	50										
N17	67.3	2.8	125	17.5	47.5	81.1	12.2	284	653	2.26	0.28	1.29	124	398.4	0.025

<b>N18</b>	82.7	2.8	125	17.5	47.5										
<b>N19</b>	75	1.2	125	17.5	47.5	67.0	119	451	902	1.74	0.38	1.32	114	236.4	0.013
<b>N20</b>	75	4.2	125	17.5	47.5	94.5	27.8	352	761	2.08	0.30	1.33	122	275.2	0.044
<b>N21</b>	75	2.8	30	17.5	47.5	74.0	3.2	241	669	2.76	0.25	1.36	133	290.4	0.011
<b>N22</b>	75	2.8	241	17.5	47.5										
<b>N23</b>	75	2.8	125	13.6	43.6	93.6	41.9	365	772	2.00	0.29	1.28	153	442.5	0.021
<b>N24</b>	75	2.8	125	21.4	51.4	91.0	91.8	380	808	1.88	0.36	1.28	97	205.3	0.018
<b>N25</b>	75	2.8	125	17.5	47.5	85.8	83.9	356	738	1.84	0.32	1.25	121	400.2	0.027
<b>N26</b>	75	2.8	125	17.5	47.5	80.5	71.3	332	713	1.93	0.32	1.25	124	411.5	0.026
<b>N27</b>	75	2.8	125	17.5	47.5	93.1	93.0	377	772	1.80	0.34	1.26	123	377.4	0.029
<b>Syloid 244</b>							1.5	3.2	7.8	1.98	0.09	1.39	296		

### 3.1 Particle surface morphology

The SEM images of some of the granules are shown in Figure 1. It can be seen that the surface of the granules is rough and that their shapes are rather irregular. It can also be seen that there are no significant or distinct differences between the selected examples, even though these granules were produced with different process parameters. This means that it is likely that the surface morphology of the granules is independent of the investigated process parameters.

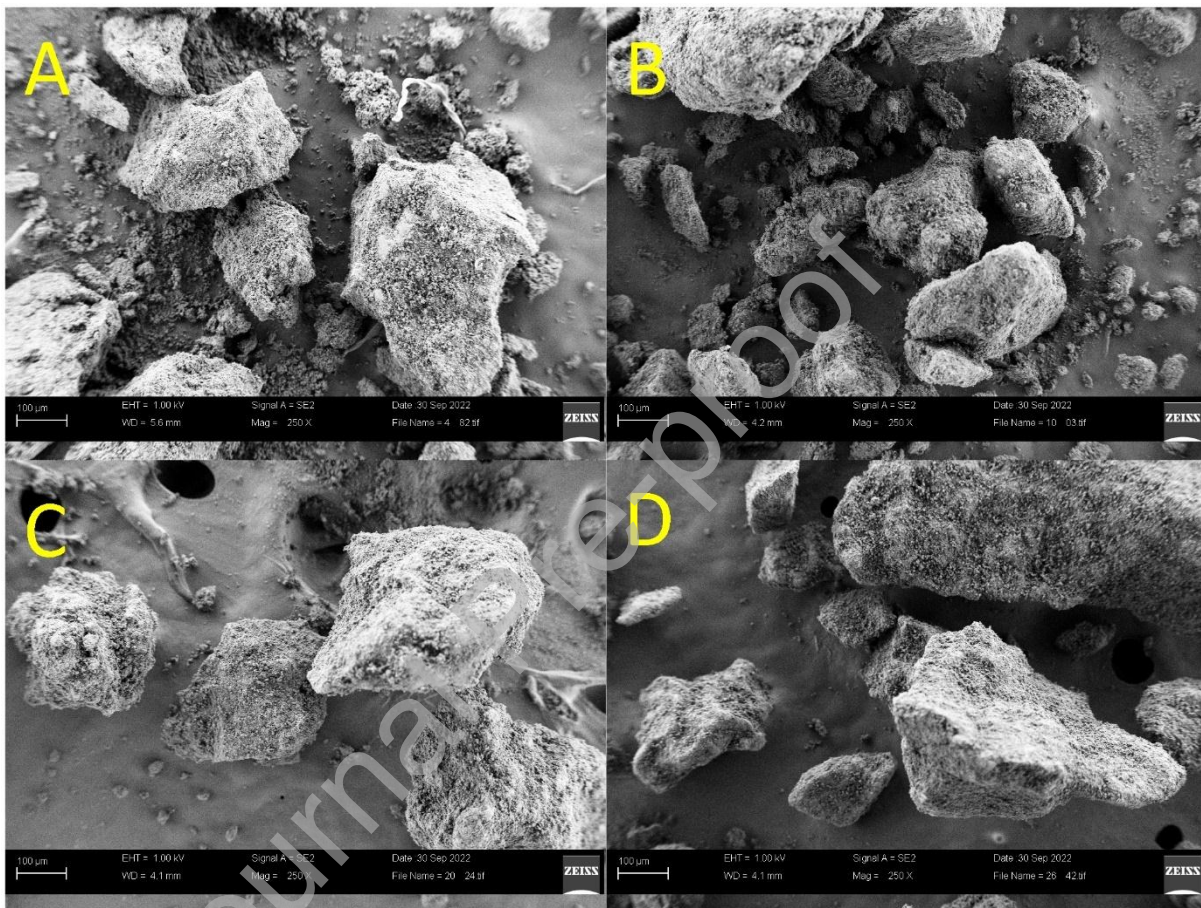


Figure 1: SEM images of N4 (A), N10 (B), N20 (C) and N26 (D)

### 3.2 DoE analysis

In the remainder of the article, responses that were undertaken for DoE analysis are presented. Since the missing cases were a consequence of overgranulation, these values were not imputed, and complete case analysis was rather performed. It has to be acknowledged that this can lead to a certain bias in estimation of factor effects. However, since granulation of small porous particles was seen to be a rather complex process, quite different from a typical granulation (e.g. large amounts of added water, relatively low impeller speed), and with many factors and their interactions in play, further analysis was undertaken despite missing cases to get at least a rough estimation of which factors are the most relevant for achieving optimal results. Parameters which were used to estimate

the quality of the generated models are shown in Table 4. Further comments on model quality will be given in separate sections.

Table 4: Parameters used to estimate the quality of the generated models

	$R^2$	$R^2$ (adjusted)	$Q^2$	Model validity	Reproducibility
<b>SSA</b>	0.87	0.86	0.84	0.23	0.99
<b>d10</b>	0.92	0.88	0.78	0.79	0.93
<b>d50</b>	0.88	0.86	0.79	0.79	0.92
<b>d90</b>	0.93	0.88	0.57	0.85	0.89
<b>span</b>	0.88	0.82	0.66	0.44	0.98
<b>Bulk density</b>	0.79	0.73	0.52	0.61	0.93
<b>Hausner ratio</b>	0.83	0.70	0.41	0.01	0.99
<b><math>P_y</math></b>	0.76	0.71	0.56	0.44	0.96
<b><math>c_p</math></b>	0.76	0.61	0.41	0.29	0.97

### 3.2.1 Effect of process parameters on specific surface area

SSA is of a critical importance in the present study, because it can have a significant effect on the adsorption of a drug onto mesoporous materials. If the characteristics of such material were appropriate for research in formulating amorphous solid dispersions of poorly water-soluble drug, SSA could play an important role in determining the amount of drug that can be adsorbed onto the material (41,42). From Table 3, it can be seen that the SSA of the granules ranged from 92 to 161  $m^2/g$ , with the most granulates ranging from 110 to 125  $m^2/g$ . Since SSA of isomalt is negligible compared to silica, theoretical SSA of the products can be calculated based only on SSA of silica and equals to 173-204  $m^2/g$ , depending on the proportion of silica in the granulate. Based on this consideration, it can be assumed that isomalt either covers or fills the pores to some extent, however, SSA of the products can still be considered high. The generated model showing the effect of process parameters on SSA is given mathematically in Equation 5:

$$SSA = 126 - 18 * bind \text{ (Eq. 5)}$$

The only parameter with a significant effect on SSA of the granulates is the amount of binder (normalized regression coefficient  $-0.93$ ). The negative sign of the regression coefficient means that higher binder amount leads to lower SSA, which is not surprising, since isomalt adsorbs to the surface of silica particles and occupies part of their surface. However, it might also be possible that there are other factors affecting SSA that were not considered in the study. The parameters used to



evaluate the quality of the model (Table 4) show high goodness of fit and predictive power. Model validity is somewhat low, but this could also be due to the very high reproducibility (40).

### 3.2.2 Effect of process parameters on particle size

Since particle size can have a significant effect on other product characteristics, especially flow and compression properties, it has been studied extensively. Mean particle size  $d_{50}$  of the granulates ranged from 207  $\mu\text{m}$  to 481  $\mu\text{m}$ , which means that granules were successfully formed in all experiments, since the starting material (Syloid 244 FP) has a mean particle size of 3.2  $\mu\text{m}$ . The parameters used to evaluate the quality of the models (Table 4) show that the goodness of fit (assessed by  $R^2$  and adjusted  $R^2$ ) is quite high in each case, and since  $Q^2$  is greater than 0.5, the models should also have good predictive power.

The effects of process parameters and their interactions on  $d_{10}$ ,  $d_{50}$ , and  $d_{90}$  are shown in Figure 2, and the mathematical descriptions of the models are given in Equations 6, 7 and 8:

$$d_{10} = 55.0 + 17.3 * w - 20.6 * war + 30.1 * imp - 9.8 * w^2 - 8.3 * w * war - 12.6 * war * imp \quad (Eq. 6)$$

$$d_{50} = 330 + 37 * w - 44 * war + 65 * imp \quad (Eq. 7)$$

$$d_{90} = 718 + 40.1 * w - 40 * war + 60 * imp + 8 * bind + 25 * war^2 - 20 * w * war + 29 * war * bind - 14 * imp * bind \quad (Eq. 8)$$

The bars in the plots represent normalized coefficients describing the magnitude and direction of the effect of a model term on a particular response. Some insignificant model terms (i.e. terms where confidence interval crosses zero) were also included in the models, either to keep them hierarchical or to obtain a higher  $R^2$  and  $Q^2$ . It is clear that impeller speed has the most significant effect on particle size (0.75, 0.84 and 0.67 for  $d_{10}$ ,  $d_{50}$  and  $d_{90}$ , respectively; normalized values). Since it has a positive direction, this implies that a higher impeller speed leads to a larger particle size. However, previous studies have shown that impeller speed can have a contrasting effect on particle size. In some cases, higher speed may lead to breakage and thus smaller particle size, but in other cases it may contribute to higher collision frequency and thus increase particle agglomeration (29,43). Furthermore, impeller speed produces compaction and shearing forces to the wet mass, and the higher these are, the larger the particles (28). The latter effects seem to be predominant in our case. The amount of water added as granulation liquid also has a significant positive effect on particle size, although this is not as prominent as for impeller speed (0.43, 0.47 and 0.45 for  $d_{10}$ ,  $d_{50}$  and  $d_{90}$ , respectively; normalized values). It has been reported before that high water amount in combination with high impeller speed account for higher liquid saturation of the granules, meaning that higher

fraction of the empty space within the granules is filled with liquid. Granules are therefore easily deformable and more liquid is available on their surface, which increases the likelihood of coalescence and agglomeration and resists separating forces caused by the impeller (29,32). However, when both factors, i.e. impeller speed and water amount, were set at high levels, this can result in an over-wet granulate as seen in Figure 3, which is not suitable for further handling. Therefore, care must be taken to ensure that both factors are not set high at the same time.

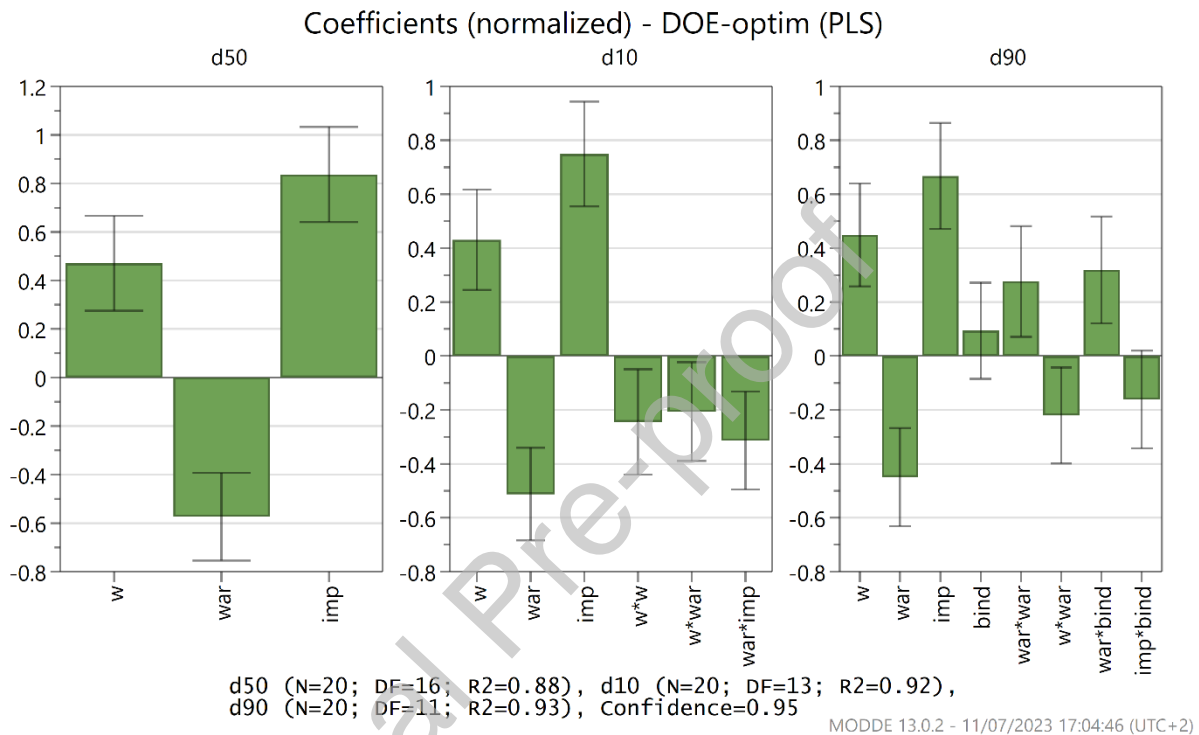


Figure 2: Coefficient plots showing effects of different factors on d50, d10, and d90.



Figure 3: Examples of overwet granulates (left: N14; right: N6)

In contrast, water addition rate seems to have a significant negative effect on particle size ( $-0.51$ ,  $-0.57$ , and  $-0.45$  for  $d_{10}$ ,  $d_{50}$  and  $d_{90}$ , respectively; normalized values). This means that water addition rate must be slower to achieve a larger particle size. The reason for this could be that with a lower water addition rate, the process time is longer and thus more time is available for granule growth. It has been previously shown that long wet massing time after complete water addition can lead to proper distribution of granulation liquid, higher liquid saturation, and thus larger particles (28,44). Wet massing was omitted in our study, because preliminary experiments showed that the probability of overwetting was significantly higher when this otherwise common step in wet granulation was performed.

Surprisingly, the amount of binder did not seem to have a significant effect on particle size in our case, although increasing the amount of binder should generally lead to larger granules (43). The reason for this could be that the values used in the experiments were too close to each other (the percentage of binder in the dry blend ranged from 32% to 42% – star points experiments). In preliminary experiments, even lower amounts of binder were used, but they did not give satisfactory results in terms of particle size and compression properties. On the other hand, further increasing the binder amount could lead to even larger particles and better compression properties, since isomalt is readily compressible (18). However, in this case, considering the model predicting SSA, the SSA of the granules would decrease even further, which is not desirable in view of the intended use of the product, i.e., for drug adsorption to prepare amorphous solid dispersions.

In the models predicting  $d_{10}$  and  $d_{90}$ , some interaction terms were also found to be significant. In both cases, the interaction between water amount and water addition rate had a negative effect on the response. This trend was also observed in the modelling of  $d_{50}$ , but in the final model this term was not significant and its inclusion would lower  $Q^2$ . The interaction plots shown in Figure 4 are commonly used to interpret the interaction terms. It can be seen that as the amount of water increases, the granule growth is less pronounced at high water addition rate, while at lower addition rate, amount of water has a greater effect on the particle size. The reason for this observation could be that if the water addition rate is too high, the process time is so fast that even with a high amount of water, there is not enough time for it to properly distribute in the blend. However, one has to be careful when explaining the interaction effects, as they are often too complex, elusive for interpretation and hardly allow clear conclusions (45).

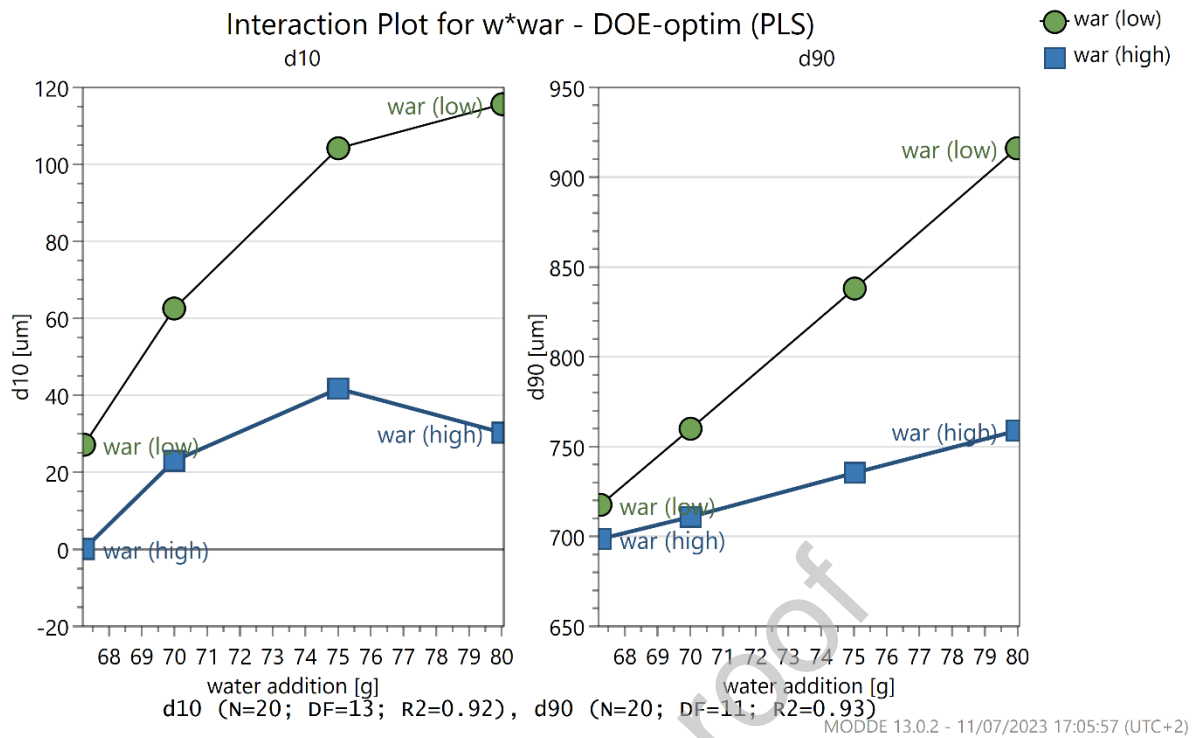


Figure 4: Interaction plot for d10 and d90 showing interaction between water amount and water addition rate.

The effect of different process parameters on particle size distribution, evaluated as span, was also studied, as it can have a significant effect on compression, flow, and segregation of the granules. It can also provide important information about the granulation process and events. In the experiments conducted, span ranged from 1.68 to 3.05, with a low value of span indicating narrow granule size distribution and vice versa (33). A visualization of the relationship between the factors affecting the span is presented as a 4D contour plot in Figure 5, and the mathematical model (Eq. 9) describing the effects of the different terms on span is as follows:

$$\text{span} = 2.13 - 0.18 * w + 0.22 * \text{war} - 0.38 * \text{imp} + 0.04 * \text{bind} + 0.08 * \text{imp}^2 + 0.12 * \text{war} * \text{bind} \quad (\text{Eq. 9})$$

It is clear that both water amount and impeller speed have a negative effect on span, meaning that higher amounts of these factors decrease it, which is in contrast to the effect that these factors have on the particle size. The same is true for water addition rate; unlike for particle size, it has a positive effect on span. The reason could be that with higher water addition rate, the granulation liquid has less time to distribute evenly in the blend, which can lead to a higher content of overwet lumps, while some areas remain drier and granule coalescence is therefore prevented there. Higher impeller speed could contribute to lower span by generating high shear forces that break overwet lumps and prevent local overwetting (29). A similar phenomenon was also observed by Fayed et al.

who reported that the narrowest granule size distribution was achieved by high water amount, high impeller speed and long wet massing time (28).

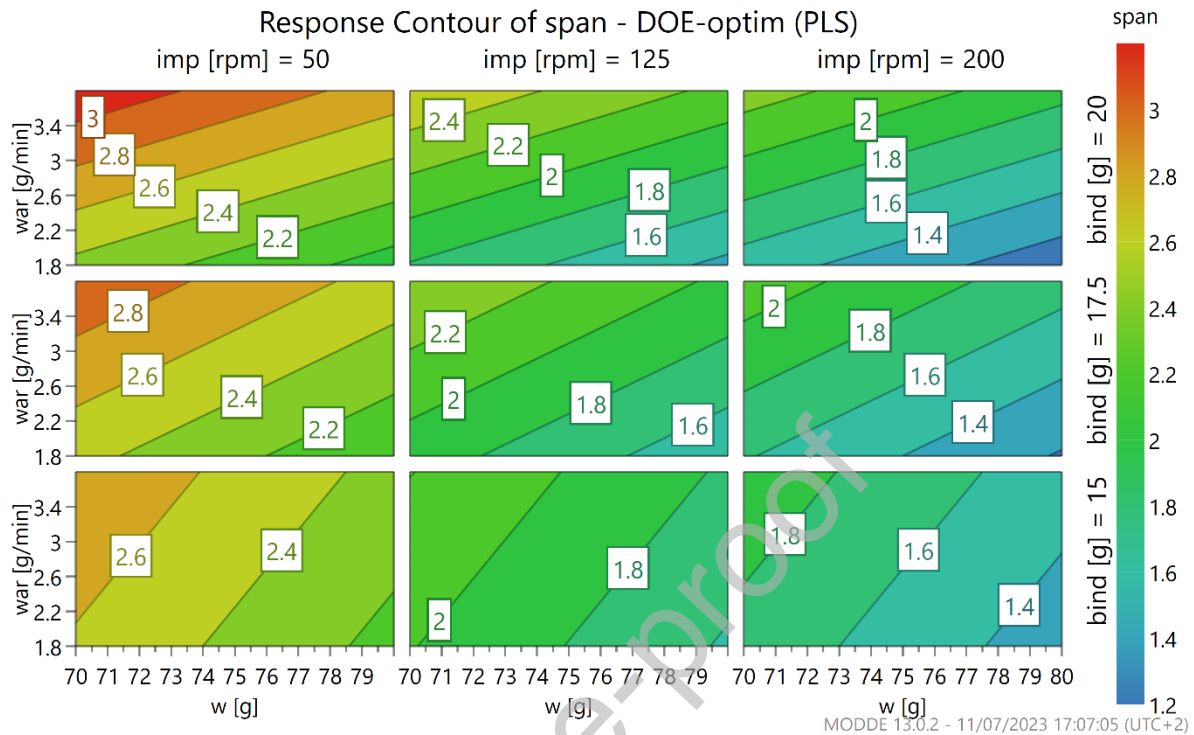


Figure 5: 4D response surface contour plot for span.

### 3.2.3 Effect of process parameters on bulk density

Like particle size, bulk density is one of the primary granulate characteristics that can have a significant impact on secondary properties such as flowability and compressibility (29,38,46). Bulk density of the prepared granulates ranged from 0.25 to 0.38 g/mL. Compared to pure Syloid 244 FP (bulk density 0.9 g/mL), it is clear that this powder property was significantly increased in each experiment. A model built to describe the effect of process variables on bulk density was linear and had good quality (Table 4). Four factors were found to be significant and were included in the model to give the highest  $Q^2$ ; amount of water, water addition rate, impeller speed and binder addition. The equation (Eq. 10) used to predict bulk density is as follows:

$$\rho_b = 0.31 + 0.02 * w - 0.02 * war + 0.03 * imp + 0.01 * bind \text{ (Eq. 10)}$$

It is clear that impeller speed has the greatest effect on granulate bulk density, followed by water amount. While these two factors as well as the amount of binder have a positive effect, the negative sign in front of water addition rate means that its higher values result in a lower bulk density. When the granules are exposed to high shear forces generated by higher impeller speed and a longer period of time as a result of slow water addition rate, their porosity decreases, while consolidation

and density increase. In fact, consolidation has been recognized as a crucial mechanism for granule density because it controls the amount of air in the granules and the rate of water coming out of the granule pores (28). It is also evident that the factors influence bulk density in the same direction as particle size. It has already been reported that a smaller granule size tends to decrease blend density due to the entrapped air and reduced packing of the granules in the powder bed, which could also at least partially explain our observations (29). Also, the correlation matrix (Table 5) presenting the correlation coefficients between the responses shows very high correlations between particle size (d10, d50, and d90) and bulk density. This means that we cannot say with certainty whether process parameters have a direct effect on bulk density or whether it is only an indirect effect via a primary particle property, i.e., particle size (47).

Table 5: Correlation matrix among responses. Blue and red colors indicate positive and negative correlations, respectively. The darker the shade, the stronger the correlation.

	SSA	d10	d50	d90	span	$\rho_b$	Hausner ratio	$P_y$	$c_p$
SSA	1.00	0.00	0.09	0.00	-0.12	-0.11	-0.12	0.76	-0.06
d10	0.00	1.00	0.89	0.83	-0.85	0.83	-0.55	0.23	-0.17
d50	0.09	0.89	1.00	0.93	-0.92	0.85	-0.60	0.25	-0.09
d90	0.00	0.83	0.93	1.00	-0.73	0.90	-0.58	0.02	-0.29
span	-0.12	-0.85	-0.92	-0.73	1.00	-0.70	0.59	-0.38	-0.15
$\rho_b$	-0.11	0.83	0.85	0.90	-0.70	1.00	-0.64	-0.03	-0.33
Hausner ratio	-0.12	-0.55	-0.60	-0.58	0.59	-0.64	1.00	-0.16	0.05
$P_y$	0.76	0.23	0.25	0.02	-0.38	-0.03	-0.16	1.00	0.07
$c_p$	-0.06	-0.17	-0.09	-0.29	-0.15	-0.33	0.05	0.07	1.00

#### 3.2.4 Effect of process parameters on flowability

Flowability is one of the bulk properties of the granulate, which is of great importance for preparation of a final dosage form such as tablet or capsule (29,48). One of the methods to evaluate it in a simple way is to determine Hausner ratio, which is calculated by Eq. 11:

$$\text{Hausner ratio} = \frac{\rho_t}{\rho_b} \quad (\text{Eq. 11}),$$

where  $\rho_t$  is tapped density of the granulate and  $\rho_b$  is its bulk density (28,34). Hausner ratio of the prepared granulates ranged from 1.18 to 1.43, with most falling into the category of “passable flowability” as defined by the European Pharmacopeia (Hausner ratio between from 1.26 to 1.43).

Hausner ratio of pure Syloid 244 FP was also measured, and considering that the result was 1.39, some of the granulates (N3, N4, N11) seem to have poorer flowability, which is contrary to what the process of granulation should lead to. However, it should be noted that Syloid 244 FP, unlike all of the granulates, was not free flowing, which was also reported by Kostelanska et al. in the test of flow through the orifice (49). It has to be emphasised that Hausner ratio is only one of the possible methods to determine flow properties of the materials. Other tests are needed to draw stronger and more accurate conclusions, and it has already been reported that different flowability methods can lead to conflicting results (21). Nevertheless, some clues as to which parameters influence Hausner ratio and, therefore, flowability of the granulates can still be seen in the DoE study. A bar chart with normalized coefficients representing the magnitude and direction of the effects on Hausner ratio can be seen in Figure 6, while Equation 12 shows mathematical representation of the model:

$$\begin{aligned} \text{Hausner ratio} = & 1.29 - 0.02 * w + 0.04 * war - 0.03 * imp + 0.02 * war^2 + 0.01 * w * war \\ & - 0.03 * war * imp - 0.02 * war * bind \text{ (Eq. 12)} \end{aligned}$$

The most significant factors determining Hausner ratio appear to be water addition rate, impeller speed, and interaction of water addition rate with impeller speed and binder amount. Not surprisingly, faster water addition rate and slower impeller speed lead to higher Hausner ratio, which corresponds to lower flowability. In fact, the same direction of these two factors leads to smaller particle size, which is often a reason for poor flow properties of a powder or granulate (27,28,50). The correlation matrix (Table 5) also shows a high negative correlation between particle size and Hausner ratio, confirming this claim. Both interaction effect plots in Figure 7 show that at lower water addition rate, higher values of the interacting factor lead to higher Hausner ratio, whereas at higher water addition rates, they lead to lower Hausner ratio. However, the precise understanding and interpretation of interaction effects can be complex (45), which is also true in this case.

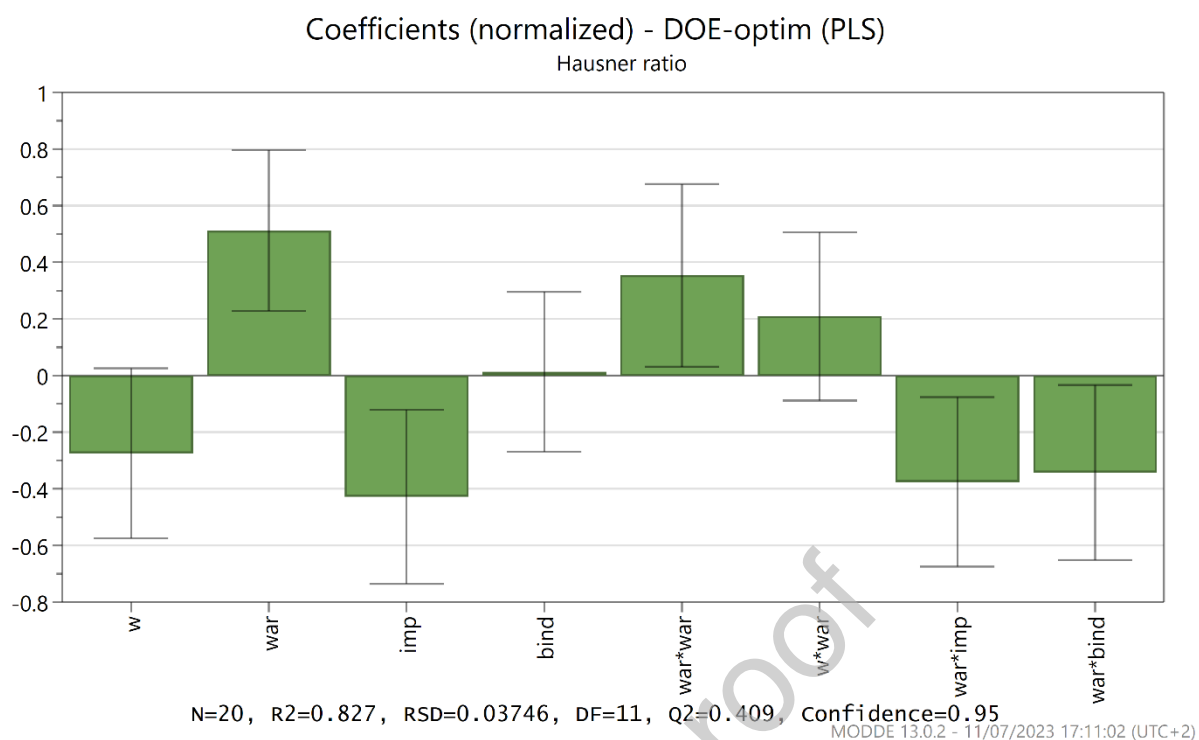


Figure 6: Coefficient plots showing effects of different factors on Hausner ratio.

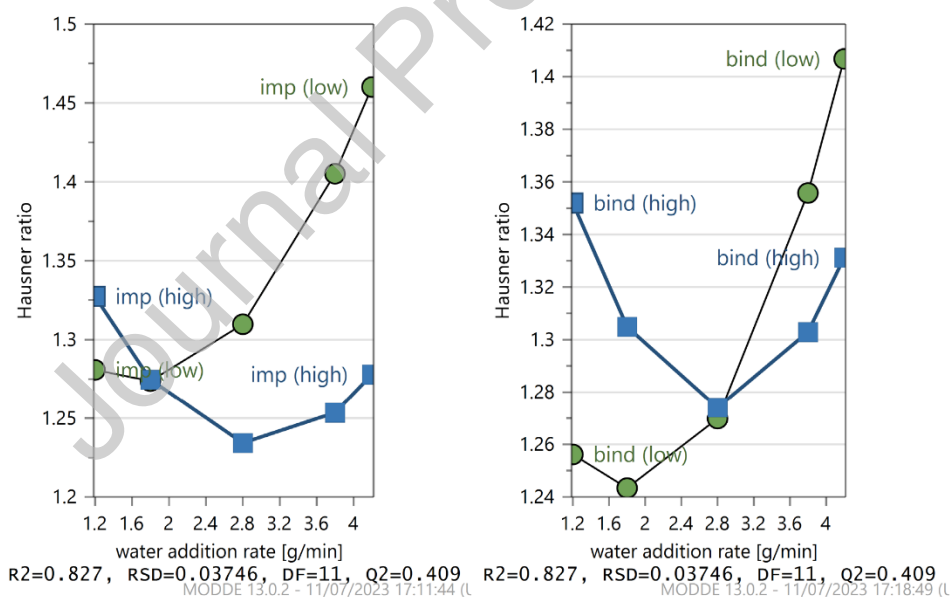


Figure 7: Interaction plots for war\*imp (left) and war\*bind (right).

The goodness of fit of the model as well as its predictive power are still satisfactory (Table 4), but the values are lower than for the previously described responses. The reason could be that Hausner ratio is a bulk property of the product, which depends on some primary particle properties, such as particle size and density. In addition, the model validity was only 0.01, which could indicate an



insignificant model. However, since the reproducibility is 0.99, the validity could also be very low due to the extremely good replicates (40). As can be seen in Figure 8, the points on the normal probability almost follow a straight line, which means that the residuals are normally distributed. Moreover, the observed responses are not far from the predicted points. These two model diagnostics plots suggest that the generated model is valid (50,51).

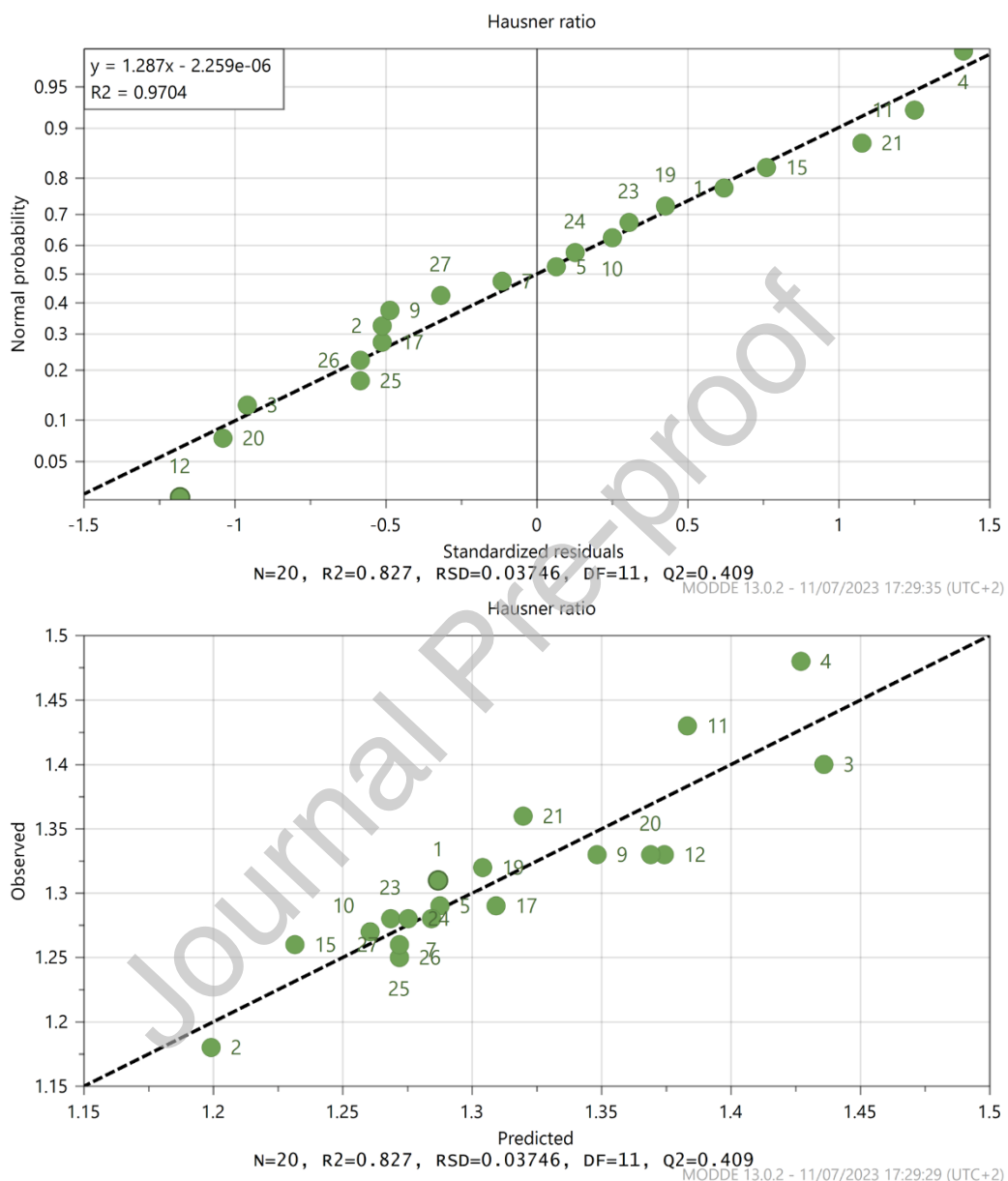


Figure 8: Residuals normal probability plot for Hausner ratio (above) and observed vs. predicted responses plot (below)

### 3.2.5 Effect of process parameters on compressibility and compactibility

Knowing compressibility and compactibility properties of the granulates is important for the production of tablets by compression, since it has already been noted that these properties are often problematic and hinder the use of tableting. Table 3 shows that both compressibility and

compactibility measures ( $P_y$  and  $c_p$ ) are not reported for pure Syloid 244 FP, because it cannot be compressed into tablets. In contrast, all of the granulates could be compressed at reasonable compaction pressures, although the tablet strength was quite low in some cases. Nevertheless, the mere fact that the granulates can be formed into tablets tells us that the characteristics of the starting material have been significantly improved by co-processing.

Looking at the parameters used to estimate the quality of the model for  $P_y$  (yield pressure) and  $c_p$  (compactibility) in Table 4, it is clear that the model quality is higher for  $P_y$  than for  $c_p$ . Considering that the compactibility model requires the calculation of radial tensile strength, which depends on tablet hardness measurement, this is not surprising, since tablet hardness is a less reliable and more variable response than, for example, tablet density, diameter, height, or mass. For  $P_y$ , the quality estimators are quite good, whereas modelling  $c_p$  resulted in a poorer model that is not expected to have high predictive significance. It also has to be noted that experiment N1 has been excluded from the model because it was recognized as an outlier, which could be a consequence of the fact that it was difficult to make tablets which did not laminate with this granulate. Equations used to predict compressibility and compactibility are as follows:

$$P_y = 366 - 22.6 * war - 71.7 * bind - 32.8 * war^2 \text{ (Eq. 13)}$$

$$c_p = 0.027 + 0.004 * w + 0.003 * imp - 0.001 * bind - 0.003 * imp^2 - 0.002 * bind^2 + 0.002 * war * imp - 0.005 * war * bind \text{ (Eq. 14)}$$

Figure 9 shows the normalized coefficients describing the magnitude and direction of the effects of each model term on  $P_y$  and  $c_p$ . Some insignificant model terms were included to keep them hierarchical or to gain higher predictive power. The most important parameter for  $P_y$  seems to be the amount of binder; the higher the amount, the lower  $P_y$ , which means that the powder is more easily consolidated under compression, i.e., has better compressibility (52). This is not surprising, since it has already been mentioned that isomalt contributes to better compressibility due to its binder properties (18,25). However, in our case, the amount of binder does not seem to have a significant effect on compactibility. For compactibility, water addition rate and impeller speed seem to have the largest influence, and both work in a positive direction; the higher the factor settings, the better compactibility. In addition, a significant interaction term was found between water addition rate and amount of binder. Its meaning is shown in Figure 10. It can be seen that water addition rate has a distinct positive effect on compactibility when the binder amount is low. On the other hand, if the binder amount is high, water addition rate has a slightly negative effect, but the importance of this effect is significantly lower than with lower binder amount.

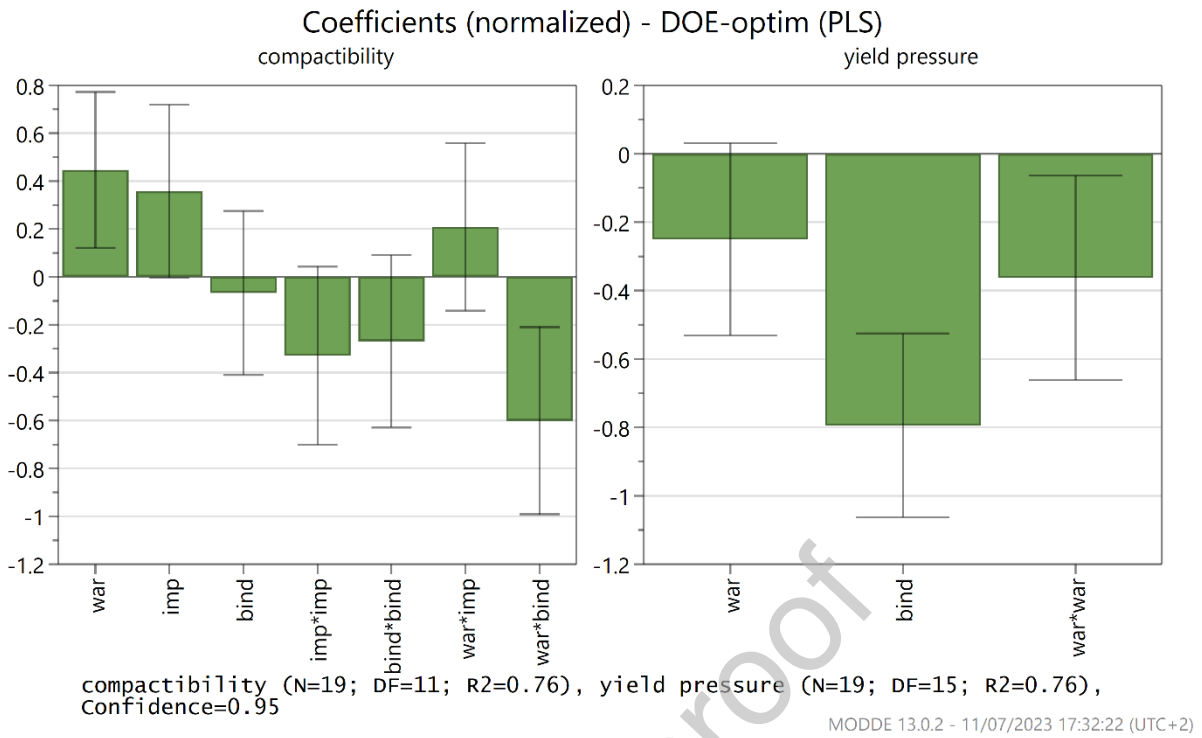


Figure 9: Coefficient plots showing effects of different factors on compactibility ( $c_p$ ) and yield pressure ( $P_y$ ).

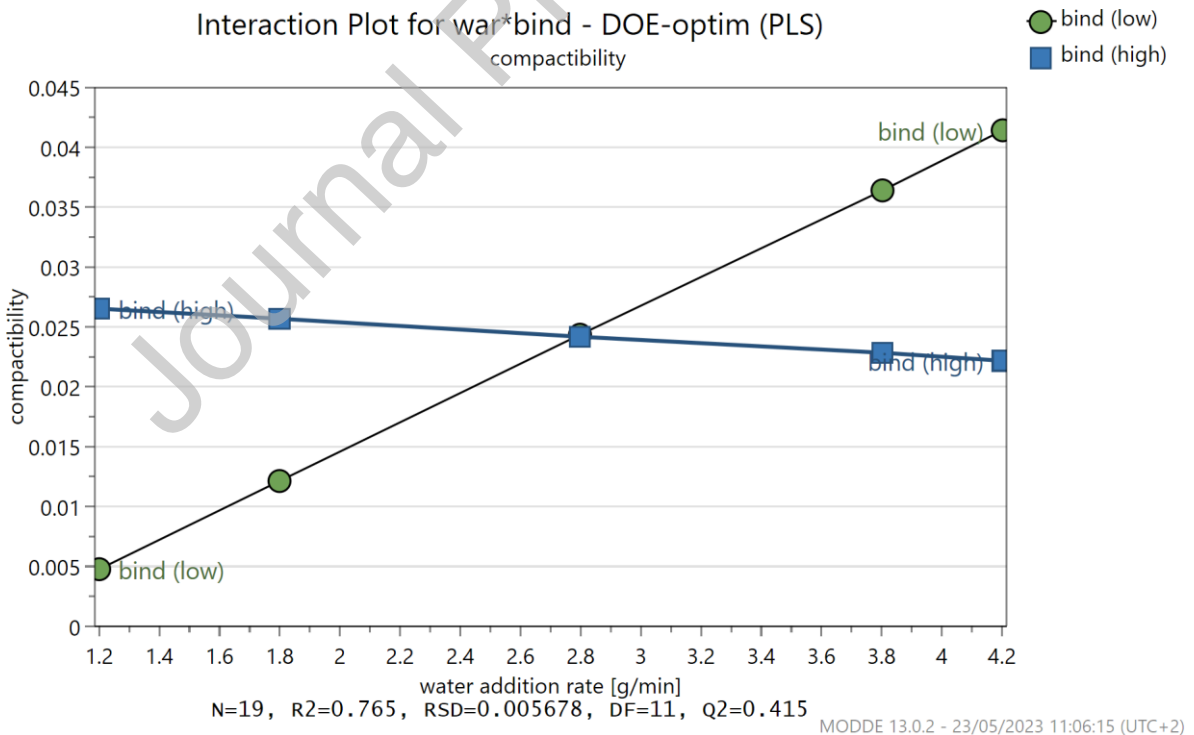


Figure 10: Interaction plots for war\*bind.

Since particle size can affect both compressibility and compactibility of the material, correlations between these parameters were also checked. A look at the correlation matrix (Table 5) shows that the correlations are all very low (absolute values below 0.3), which means that, at least in this case, particle size does not seem to be related to compression and compaction properties. From the literature, it appears that there is no single rule for the influence of particle size on compressibility and compactibility and that sometimes these characteristics seem to be independent, while in other cases, correlations have been observed (38,53,54). In our case, further studies would be needed to provide more reliable models to draw stronger conclusions about the influence of particle size on compression and compaction properties, or lack thereof.

### 3.2.6 Optimization experiments

The goal of the optimization experiments was to obtain materials with the most desired chosen characteristics (high SSA, big particle size, good flow and compression properties) and to confirm the validity of our models. Considering this, as the model quality for  $c_p$  was quite poor to start with,  $c_p$  was omitted from optimization. The process parameters for the two optimization experiments, obtained using the Modde® software response optimizer, are listed in Table 7. Some factor constraints were applied in order to avoid overwetting of the granulates and too long process duration; water amount was therefore limited at 75 g and impeller speed at 125 rpm, while the water addition rate was limited to a minimum of 1.8 g/min.

Table 7: Factor settings for optimization experiments

Factor	Unit	OPT 1	OPT 2
Isomalt amount	g	13.6	21.4
Water amount	g	74.8	71.4
Water addition rate	g/min	1.8	4.2
Impeller speed	rpm	125	65

In optimization experiment #1 (OPT 1), both d50 (mean particle size) and SSA were optimized to a maximum value. Both responses were optimized simultaneously, because their generated DoE models contained different factors, meaning that changing the factor settings influenced one response at a time. The measured SSA was 141 m<sup>2</sup>/g. Compared with the response predicted by the optimizer, which was 156 m<sup>2</sup>/g, the difference is less than 10%, and furthermore, the goodness of fit and predictive power of the model remained very high (R<sup>2</sup> 0.85, adjusted R<sup>2</sup> 0.84, Q<sup>2</sup> 0.82).

As mentioned before, SSA is an important parameter to be considered for the feasibility of subsequent drug loading and amorphization, but it is not the only parameter that governs this

process in mesoporous materials. In fact, total pore volume and average pore size could also play an important role (55,56). Therefore these properties were also measured in the starting material, i.e. Syloid 244 FP, and in product "OPT 1". The full adsorption and desorption isotherms are given in Figure 11. Total pore volume of pores less than 40 nm wide decreased from 1.6 mL/g to 0.8 mL/g, while average pore size decreased from 9.3 nm to 7.1 nm. This indicates that isomalt filled larger pores to a certain extent, which is not an optimal result and suggests that further improvements could be made to achieve greater pore volume as well as greater SSA. However, half of the initial pore volume remained unfilled and SSA was still quite large, which can still be considered promising for further research.

Journal Pre-proof

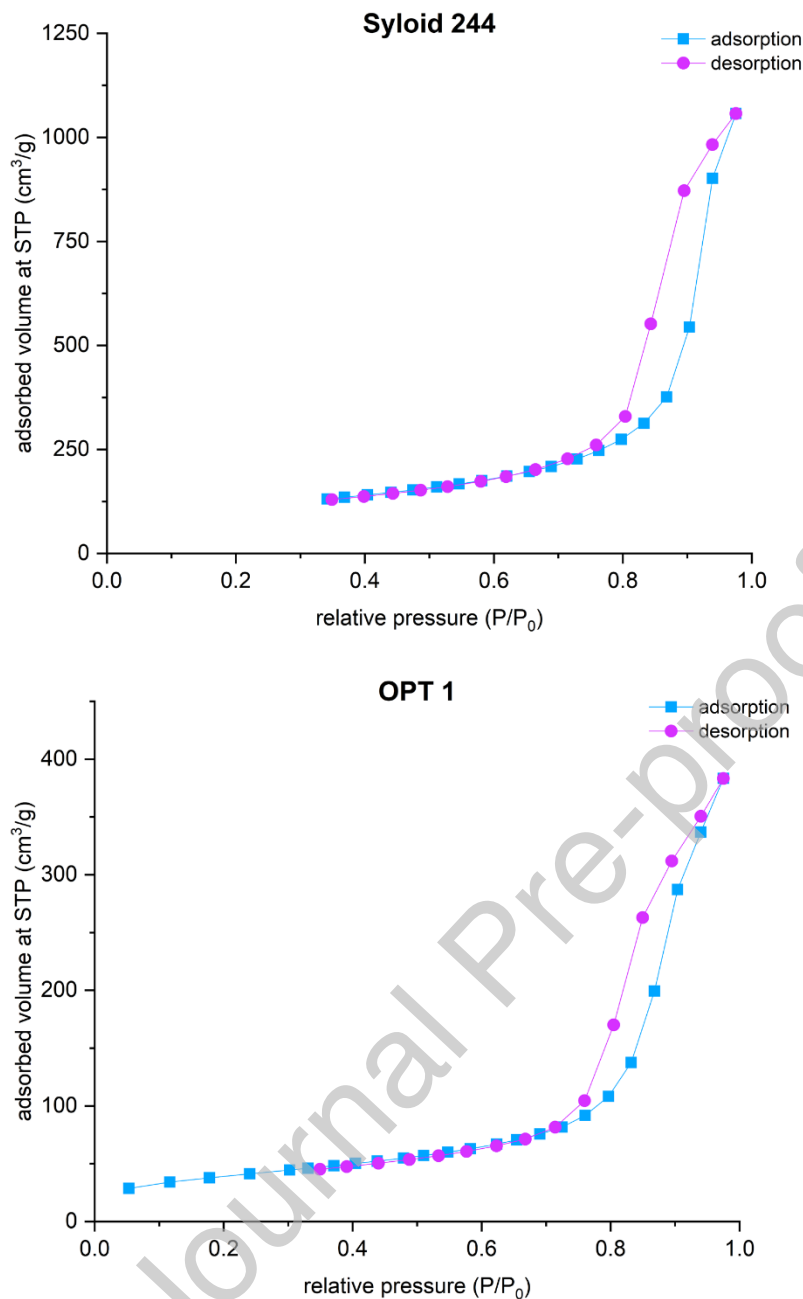


Figure 11: Adsorption and desorption isotherms of Syloid 244 (upper figure) and OPT 1 (lower figure)

The measured d50 of “OPT 1” was 380  $\mu\text{m}$ , while the response optimizer predicted 416  $\mu\text{m}$ . Although the actual d50 value is slightly lower than the predicted one, the difference is again less than 10% and when fitted to the model, the model quality parameters even improved by little ( $R^2$  0.89 vs. 0.88, adjusted  $R^2$  0.87 vs 0.86,  $Q^2$  0.80 vs. 0.79), also confirming the validity of our model. Since particle size was previously found to also affect bulk density and flowability (indicated by Hausner ratio), these two responses were also measured and compared to the predicted values. Bulk density was 0.30 g/mL (predicted value 0.34 g/mL) and Hausner ratio was 1.27 (predicted value 1.23). Since particle size was slightly lower than the predicted value, these deviations were to be

expected. Nevertheless, it can be said that the actual values are quite close to predicted values and that particle size optimization can also be used to optimize these two characteristics. Since their models do not have such high model quality estimators, it makes sense to optimize  $d_{50}$  instead. When these results from OPT 1 were added to the models, the model quality parameters remained the same (Hausner ratio) or were decreased (bulk density), but only by little ( $R^2$  0.78 vs. 0.79, adjusted  $R^2$  0.72 vs. 0.73,  $Q^2$  0.42 vs. 0.52), which also gives a higher significance to these models.

In optimization experiment #2 (OPT 2),  $P_y$  was optimized to a minimum value, implying better compressibility. The  $P_y$  of the compressed granulate, which was calculated using the Heckel compressibility model, was 211.3 MPa. Compared to the predicted response of 140.5 MPa, it can be said that the difference is quite high. However, considering that the quality parameters of the model predicting  $P_y$  were not as good as those of the models predicting particle size or SSA, this finding is somewhat expected. When the value of OPT 2 was added to the model, quality parameters of the model remained more or less the same or even slightly increased (adjusted  $R^2$  0.72 vs. 0.71,  $Q^2$  0.60 vs. 0.56), which means that the experiment confirmed and even slightly improved our model.

#### 4 Conclusions

Mesoporous silica was successfully granulated with isomalt as a binder to form a novel co-processed excipient that was expected to have better flow and compression properties than the starting material, while maintaining high specific surface area. Granulate properties (particle morphology, SSA, particle size, particle size distribution) and bulk properties (bulk density, flowability, compressibility and compactibility) were evaluated and shown to comply with the aim of the study. The effects of process parameters in high-shear granulation on characteristics of this co-processed excipient were successfully studied using a DoE approach and models for each response were generated. Goodness of fit and predictive power of the models were mostly good ( $R^2$  above 0.7,  $Q^2$  mostly above 0.5). However, models for particle properties generally showed higher quality than models for bulk properties, and furthermore, the latter can actually often be dependent on particle properties, as confirmed by the correlation matrix. The undertaken optimization experiments confirmed the validity of the generated models and were more or less in agreement with the predicted values, but again, more accurate results were achieved when optimizing particle properties compared to optimization of bulk properties. The developed and optimized co-processed excipient holds good potential for investigating the feasibility of loading different APIs to formulate amorphous solid dispersions that could be compressed directly. Should these predictions be accurate, it would offer a good platform to address the challenge of poor water solubility as well as the complexity associated with developing a simple and cost-effective manufacturing process for the final dosage form.

## 5 References

1. Saha S, Shahiwala AF. Multifunctional coprocessed excipients for improved tableting performance. *Expert Opin Drug Deliv*. 2009 Feb;6(2):197–208.
2. Jivraj II, Martini LG, Thomson CM. An overview of the different excipients useful for the direct compression of tablets. *Pharm Sci Technol Today*. 2000 Feb;3(2):58–63.
3. Franc A, Vetchý D, Vodáčková P, Kubařák R, Jendryková L, Goněc R. Co-processed excipients for direct compression of tablets. *Ceska Slov Farm Cas Ceske Farm Spolecnosti Slov Farm Spolecnosti*. 2018 Dec 18;67(5–6):175–81.
4. Bowles BJ, Dziemidowicz K, Lopez FL, Orlu M, Tuleu C, Edwards AJ, et al. Co-Processed Excipients for Dispersible Tablets–Part 1: Manufacturability. *AAPS PharmSciTech*. 2018 Aug 1;19(6):2598–609.
5. Li XH, Zhao LJ, Ruan KP, Feng Y, Xu DS, Ruan KF. The application of factor analysis to evaluate deforming behaviors of directly compressed powders. *Powder Technol*. 2013 Oct 1;247:47–54.
6. Jain S. Mechanical properties of powders for compaction and tableting: an overview. *Pharm Sci Technol Today*. 1999 Jan;2(1):20–31.
7. Gohel MC, Jogani PD. A review of co-processed directly compressible excipients. *J Pharm Pharm Sci Publ Can Soc Pharm Sci Soc Can Sci Pharm*. 2005 Apr 16;8(1):76–93.
8. Garg N, Dureja H, Kaushik D. Co-processed excipients: a patent review. *Recent Pat Drug Deliv Formul*. 2013 Apr;7(1):73–83.
9. The International Pharmaceutical Council. Co-processed Excipient Guide For Pharmaceutical Excipients [Internet]. The International Pharmaceutical Excipient Council; 2017 [cited 2022 Sep 21]. Available from: [https://www.gmp-compliance.org/files/guidemgr/20171030\\_Co-processed\\_Excipient\\_Guide\(FINAL\\_FOR\\_PUBLICATION\).pdf](https://www.gmp-compliance.org/files/guidemgr/20171030_Co-processed_Excipient_Guide(FINAL_FOR_PUBLICATION).pdf)
10. Dziemidowicz K, Lopez FL, Bowles BJ, Edwards AJ, Ernest TB, Orlu M, et al. Co-Processed Excipients for Dispersible Tablets–Part 2: Patient Acceptability. *AAPS PharmSciTech*. 2018 Aug;19(6):2646–57.
11. Mehra D, Kenneth P. West, J. Donald Wiggins. Coprocessed microcrystalline cellulose and calcium carbonate composition and its preparation [Internet]. US4744987A. Available from: <https://patents.google.com/patent/US4744987A/en>
12. Cellactose 80 [Internet]. [cited 2022 Sep 21]. Available from: <https://www.pharmaexcipients.com/product/cellactose-80/>
13. Ludipress® [Internet]. [cited 2022 Sep 21]. Available from: <https://pharma.basf.com/products/ludipress>
14. StarLac® [Internet]. [cited 2022 Sep 21]. Available from: <https://www.meggle-pharma.com/en/lactose/14-starlac.html>
15. Ludiflash® [Internet]. [cited 2022 Sep 21]. Available from: <https://pharma.basf.com/products/ludiflash>
16. BASF. Ludiflash®. 2019.

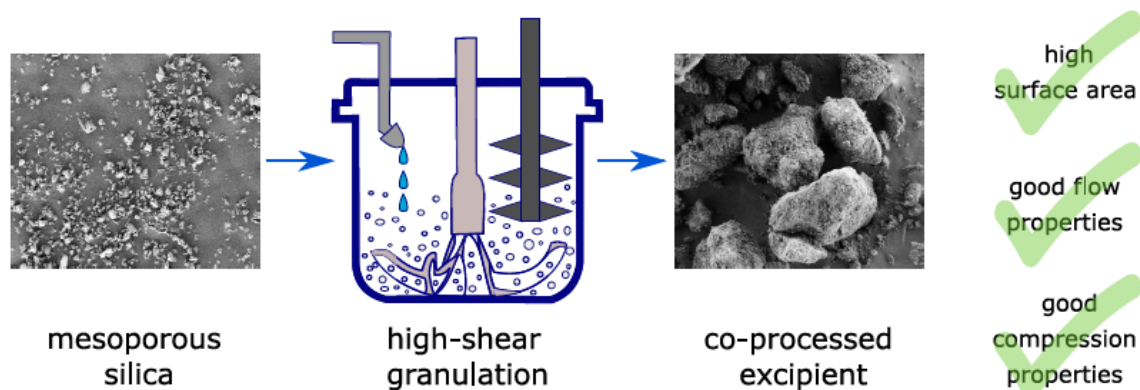


17. SPI Pharma. Pharmaburst® 500 [Internet]. [cited 2022 Sep 21]. Available from: <https://www.spipharma.com/media/3307/pharmaburst-sell-sheet-final.pdf>
18. Sáska Zs, Dredán J, Balogh E, Luhn O, Shafir G, Antal I. Effect of isomalt as novel binding agent on compressibility of poorly compactable paracetamol evaluated by factorial design. *Powder Technol.* 2010 Jul 26;201(2):123–9.
19. Chaudhari SP, Gupte A. Mesoporous Silica as a Carrier for Amorphous Solid Dispersion. *Br J Pharm Res.* 2017;16:1–19.
20. Kawabata Y, Wada K, Nakatani M, Yamada S, Onoue S. Formulation design for poorly water-soluble drugs based on biopharmaceutics classification system: basic approaches and practical applications. *Int J Pharm.* 2011 Nov 25;420(1):1–10.
21. Vialpando M, Albertini B, Passerini N, Bergers D, Rombaut P, Martens JA, et al. Agglomeration of mesoporous silica by melt and steam granulation. Part I: a comparison between disordered and ordered mesoporous silica. *J Pharm Sci.* 2013 Nov;102(11):3966–77.
22. Vialpando M, Albertini B, Passerini N, Heyden YV, Rombaut P, Martens JA, et al. Agglomeration of Mesoporous Silica by Melt and Steam Granulation. Part II: Screening of Steam Granulation Process Variables Using a Factorial Design. *J Pharm Sci.* 2013 Nov 1;102(11):3978–86.
23. Iveson SM, Litster JD, Hapgood K, Ennis BJ. Nucleation, growth and breakage phenomena in agitated wet granulation processes: a review. *Granulation Coat Fine Powders.* 2001 Jun 4;117(1):3–39.
24. Vialpando M, Backhuijs F, Martens JA, Van den Mooter G. Risk assessment of premature drug release during wet granulation of ordered mesoporous silica loaded with poorly soluble compounds itraconazole, fenofibrate, naproxen, and ibuprofen. *Eur J Pharm Biopharm.* 2012 May 1;81(1):190–8.
25. Bolhuis GK, Rexwinkel EG, Zuurman K. Polyols as filler-binders for disintegrating tablets prepared by direct compaction. *Drug Dev Ind Pharm.* 2009 Jun;35(6):671–7.
26. Conceição L, Bogel-Lukasik E, Lukasik R. A New Outlook on Solubility of Carbohydrates and Sugar Alcohols in Ionic Liquids. *Rsc Adv.* 2012 Feb 13;2:1846–55.
27. Baumgartner A, Planinšek O. Application of commercially available mesoporous silica for drug dissolution enhancement in oral drug delivery. *Eur J Pharm Sci Off J Eur Fed Pharm Sci.* 2021 Dec 1;167:106015.
28. Fayed MH, Abdel-Rahman SI, Alanazi FK, Ahmed MO, Tawfeek HM, Al-Shdefat RI. New gentle-wing high-shear granulator: impact of processing variables on granules and tablets characteristics of high-drug loading formulation using design of experiment approach. *Drug Dev Ind Pharm.* 2017 Oct;43(10):1584–600.
29. Badawy SIF, Narang AS, LaMarche K, Subramanian G, Varia SA. Mechanistic basis for the effects of process parameters on quality attributes in high shear wet granulation. *Int J Pharm.* 2012 Dec 15;439(1):324–33.
30. Kayrak-Talay D, Dale S, Wassgren C, Litster J. Quality by design for wet granulation in pharmaceutical processing: Assessing models for a priori design and scaling. *Powder Technol.* 2013 May 1;240:7–18.

31. Ohno I, Hasegawa S, Yada S, Kusai A, Moribe K, Yamamoto K. Importance of evaluating the consolidation of granules manufactured by high shear mixer. *Int J Pharm.* 2007 Jun 29;338(1–2):79–86.
32. Badawy SIF, Menning MM, Gorko MA, Gilbert DL. Effect of process parameters on compressibility of granulation manufactured in a high-shear mixer. *Int J Pharm.* 2000 Mar 30;198(1):51–61.
33. Vemavarapu C, Surapaneni M, Hussain M, Badawy S. Role of drug substance material properties in the processibility and performance of a wet granulated product. *Int J Pharm.* 2009 Jun 5;374(1–2):96–105.
34. Council of Europe. *European Pharmacopoeia 10th Edition.* Strasbourg: Council of Europe; 2019.
35. Brunauer S, Emmett PH, Teller E. Adsorption of Gases in Multimolecular Layers. *J Am Chem Soc.* 1938 Feb 1;60(2):309–19.
36. Lippens BC, de Boer JH. Studies on pore systems in catalysts: V. The t method. *J Catal.* 1965 Jun 1;4(3):319–23.
37. Barrett EP, Joyner LG, Halenda PP. The Determination of Pore Volume and Area Distributions in Porous Substances. I. Computations from Nitrogen Isotherms. *J Am Chem Soc.* 1951 Jan 1;73(1):373–80.
38. Šantl M, Ilić I, Vrečer F, Baumgartner S. A compressibility and compactibility study of real tableting mixtures: the effect of granule particle size. *Acta Pharm Zagreb Croat.* 2012 Nov;62(3):325–40.
39. Montgomery D. *Design and Analysis of Experiments.* New York, NY, USA: John Wiley & Sons; 2001.
40. Modde 12 User Guide [Internet]. Sartorius; 2017 [cited 2022 Jul 11]. Available from: <https://www.sartorius.com/download/544636/modde-12-user-guide-en-b-00090-sartorius-data.pdf>
41. Maleki A, Kettiger H, Schoubben A, Rosenholm JM, Ambrogi V, Hamidi M. Mesoporous silica materials: From physico-chemical properties to enhanced dissolution of poorly water-soluble drugs. *J Controlled Release.* 2017 Sep 28;262:329–47.
42. Le TT, Elzhry Elyafi AK, Mohammed AR, Al-Khattawi A. Delivery of Poorly Soluble Drugs via Mesoporous Silica: Impact of Drug Overloading on Release and Thermal Profiles. *Pharmaceutics.* 2019 Jun 10;11(6).
43. Oka S, Kašpar O, Tokárová V, Sowrirajan K, Wu H, Khan M, et al. A quantitative study of the effect of process parameters on key granule characteristics in a high shear wet granulation process involving a two component pharmaceutical blend. *Adv Powder Technol.* 2015 Jan 1;26(1):315–22.
44. Pandey P, Tao J, Chaudhury A, Ramachandran R, Gao JZ, Bindra DS. A combined experimental and modeling approach to study the effects of high-shear wet granulation process parameters on granule characteristics. *Pharm Dev Technol.* 2013 Feb 1;18(1):210–24.

45. Videc D, Planinšek O, Lamešič D. Design of Experiments for Optimization of the Lactose Spherical Crystallization Process. *J Pharm Sci.* 2020 Sep 1;109(9):2774–86.
46. Suresh P, Sreedhar I, Vaidhiswaran R, Venugopal A. A comprehensive review on process and engineering aspects of pharmaceutical wet granulation. *Chem Eng J.* 2017 Nov 15;328:785–815.
47. Kay, Phil. Why design experiments? Reason 4: Clarity [Internet]. [cited 2022 Sep 29]. Available from: <https://community.jmp.com/t5/JMP-Blog/Why-design-experiments-Reason-4-Clarity/ba-p/58650>
48. Pohlen M, Lavrič Z, Prestidge C, Dreu R. Preparation, Physicochemical Characterisation and DoE Optimisation of a Spray-Dried Dry Emulsion Platform for Delivery of a Poorly Soluble Drug, Simvastatin. *AAPS PharmSciTech.* 2020 Apr 21;21(4):119.
49. Kostelanská K, Prudilová BB, Holešová S, Vlček J, Vetchý D, Gajdziok J. Comparative Study of Powder Carriers Physical and Structural Properties. *Pharmaceutics.* 2022 Apr 8;14(4).
50. Almutairy BK, Khafagy ES, Alalaiwe A, Aldawsari MF, Alshahrani SM, Alsulays BB, et al. Enhancing the Poor Flow and Tableting Problems of High Drug-Loading Formulation of Canagliflozin Using Continuous Green Granulation Process and Design-of-Experiment Approach. *Pharm Basel Switz.* 2020 Dec 17;13(12).
51. Analysis of Residuals explained [Internet]. 2018 [cited 2022 Jul 20]. Available from: <https://opexresources.com/analysis-residuals-explained/>
52. Zhang J, Wu CY, Pan X, Wu C. On Identification of Critical Material Attributes for Compression Behaviour of Pharmaceutical Diluent Powders. *Materials.* 2017 Jul 23;10:845.
53. Badawy SIF, Gray DB, Hussain MA. A Study on the Effect of Wet Granulation on Microcrystalline Cellulose Particle Structure and Performance. *Pharm Res.* 2006 Mar 1;23(3):634–40.
54. Shi L, Feng Y, Sun CC. Roles of granule size in over-granulation during high shear wet granulation. *J Pharm Sci.* 2010 Aug;99(8):3322–5.
55. Xu W, Riikonen J, Lehto VP. Mesoporous systems for poorly soluble drugs. *Int J Pharm.* 2013 Aug 30;453(1):181–97.
56. Heikkilä T, Salonen J, Tuura J, Kumar N, Salmi T, Murzin DY, et al. Evaluation of mesoporous TCPSi, MCM-41, SBA-15, and TUD-1 materials as API carriers for oral drug delivery. *Drug Deliv.* 2007 Aug;14(6):337–47.

## Graphical abstract



## Formatting of funding sources

This research was co-funded by the Slovenian Research Agency (research core funding P1-0189).

## Acknowledgements

The authors gratefully acknowledge the financial support provided by the Slovenian Research Agency (Program Code P1-0189). We also acknowledge Carolina Araújo and Andreia Santos from Coimbra Health School in Portugal for their help with the experimentation.

## CRediT authorship contribution statement

**Odon Planinšek:** Conceptualization, Methodology, Investigation, Writing - review & editing, Supervision, Validation, Project administration, Funding acquisition. **Ana Baumgartner:** Methodology, Formal analysis, Investigation, Data curation, Writing - original draft, Visualisation,

## Declaration of Competing Interest

The authors declare that they have no conflicts of interest.